Pilot-Less High-Rate Block Transmission with Two-Dimensional Basis Expansion Model for Doubly-Selective Fading MIMO Systems

Koike-Akino, Toshiaki; Orlik, Philip V.; Kim, Kyeong Jin

Abstract

We investigate non-coherent multi-antenna signal processing which requires no channel state information (CSI) at either transmitter or receiver ends. With non-coherent constellations over Grassmannian manifold, a receiver employing generalized likelihood ratio test (GLRT) algorithm offers the maximum-likelihood performance even without CSI. The conventional GLRT relies on the assumption that the wireless channel is time-invariant during a block. We propose an improved GLRT algorithm which employs a novel two-dimensional basis expansion model (2D-BEM) to cope with doubly-selective fading channels. The proposed method uses sequential GLRT for multisymbol detection to keep high performance yet low complexity. Furthermore, we introduce Fourier-Legendre product basis to be robust against hardware impairments including carrier frequency and timing offsets. We demonstrate that the proposed scheme significantly improves performance in rapid fading channels, and realizes highly spectrum-efficient transmission up to 6 bps/Hz without any pilots.

Pilot-Less High-Rate Block Transmission with Two-Dimensional Basis Expansion Model for Doubly-Selective Fading MIMO Systems

Toshiaki Koike-Akino, Philip V. Orlik, Keyong Jin Kim
Mitsubishi Electric Research Laboratories (MERL), 201 Broadway, Cambridge, MA 02139, USA
Email: {koike, porlik, kkim}@merl.com

Abstract—We investigate non-coherent multi-antenna signal processing which requires no channel state information (CSI) at either transmitter or receiver ends. With non-coherent constellations over Grassmannian manifold, a receiver employing generalized likelihood ratio test (GLRT) algorithm offers the maximum-likelihood performance even without CSI. The conventional GLRT relies on the assumption that the wireless channel is time-invariant during a block. We propose an improved GLRT algorithm which employs a novel two-dimensional basis expansion model (2D-BEM) to cope with doubly-selective fading channels. The proposed method uses sequential GLRT for multi-symbol detection to keep high performance yet low complexity. Furthermore, we introduce Fourier–Legendre product basis to be robust against hardware impairments including carrier frequency and timing offsets. We demonstrate that the proposed scheme significantly improves performance in rapid fading channels, and realizes highly spectrum-efficient transmission up to 6 bps/Hz without any pilots.

I. INTRODUCTION

A large number of studies in the past decade have proven that the use of multiple antennas at both transmitter and receiver, known as multi-input multi-output (MIMO) systems, can dramatically improve spectral efficiency. In rich-scattering channel environment, the link capacity asymptotically increases as a linear function of $\min(M, N)$ [1,2], where M and N denote the number of transmitting antennas and that of receiving antennas, respectively. More recently, it motivates the use of very large number (e.g., hundreds) of antennas in the context of massive MIMO [3,4]. To achieve multiplexing gains and/or antenna diversity gains, accurate channel state information (CSI) is necessary for *coherent* communications [5–8]. In practice, CSI is obtained by transmitting pre-defined training signals or pilots. However, it is not always advantageous to use such pilot-based schemes, in particular for the case when the channel rapidly changes [9, 10]. Moreover, one of major challenges to realize massive MIMO systems includes so-called *pilot contamination* [11–15], where overheads of orthogonal pilots to support massive antennas can constrain the system throughput.

In ultra-fast fading channels for mobile radio systems including bullet train and vehicular communications, the time-varying channel fluctuation creates difficulty for both transmitter and receiver in acquiring accurate CSI, that may necessitate *non-coherent* communications. Some theoretical works [16–21] have verified that the non-coherent channel capacity

increases with $M'(1 - M'/L)$ in the high signal-to-noise ratio (SNR) regimes, where $M' = \min(M, N, \lfloor L/2 \rfloor)$ and L denotes the coherence time (or, the length of non-coherent codes) with $\lfloor x \rfloor$ being the floor function. Those theoretical studies have motivated several works on signal design of non-coherent codes, which include unitary space-time modulations (USTM) [22–37]. Such a non-coherent transmission has been considered a viable countermeasure of pilot contamination [13] as an alternative of other pilot-decontamination techniques [14, 15].

Marzetta and Hochwald showed in [16] that USTM asymptotically achieves the non-coherent channel capacity in some specific cases. Further theoretical analyses [17–19] followed, in particular, Zheng and Tse derived the non-coherent channel capacity for more general cases in [17]. For USTM, optimal performance of maximum-likelihood decoding can be offered by a receiving algorithm called generalized likelihood ratio test (GLRT) [38] even without CSI. The key idea behind the GLRT receiver lies in the fact that it employs implicit channel estimation for each codeword of the non-coherent space-time codebook at the same time of decoding. However, the conventional GLRT may suffer from a severe performance degradation when the channel coherence time is mush shorter than the length of non-coherent codes L for time-varying fading channels. Hence, the code length is generally constrained to be reasonably short in practice. The short space-time codes in turn decrease the capacity gains of $M'(1 - M'/L)$. In [39], the authors proposed an improved GLRT receiver which introduced *virtual codebook* for multi-symbol detection and basis expansion model (BEM) [40, 41], in order to deal with the above-mentioned tradeoff between performance and the code length for any coherence time. In time-varying fast fading, the virtual codebook can significantly improve the original GLRT receiver. However, realizing non-coherent transmission to achieve more than 2 bps/Hz is still challenging with a few antennas in particular for doubly-selective fading channels

In this paper, we propose an improved blind receiver algorithm employing two-dimensional (2D) BEM to realize non-coherent transmission achieving high spectral efficiency up to 6 bps/Hz even in the presence of 5% Doppler spread and 5% delay spread. The proposed method is based on the Viterbi algorithm with per-survivor processing (PSP) to efficiently decode consecutive space-time block codes. In this

paper, we demonstrate that our proposed scheme offers a significant improvement in error rate performance for non-coherent MIMO systems with orthogonal frequency-division multiplexing (OFDM). In addition, we introduce Fourier–Legendre product basis for 2D-BEM to be robust against hardware imperfections with carrier frequency offset and timing offset. The major contributions of this paper are summarized as follows:

- We propose an improved GLRT algorithm by using 2D-BEM to mitigate the penalty due to doubly-selective fading channels.
- We introduce PSP with M-algorithm to keep computational complexity low regardless of the codeword length for successive multi-symbol detection.
- We use Fourier–Legendre convolution basis for 2D-BEM to be robust against carrier frequency offset and timing offset.
- We demonstrate that the proposed method achieves high spectral efficiency up to 6 bps/Hz in the presence of strong interference in 5% Doppler spread and 5% delay spread as well as 2% carrier frequency offset and 10% timing offset.

Notations: Throughout the paper, we describe matrices and vectors by bold-face italic letters in capital cases and small cases, respectively. Let $\boldsymbol{X} \in \mathbb{C}^{m \times n}$ be a complex-valued $(m \times n)$-dimensional matrix, where $\mathbb{C}$ denotes the complex field. The notations $[\boldsymbol{X}]_{m:n}$, $\boldsymbol{X}^*$, $\boldsymbol{X}^{\mathrm{T}}$, $\boldsymbol{X}^\dagger$, $\boldsymbol{X}^{-1}$, $\mathrm{tr}[\boldsymbol{X}]$ and $\|\boldsymbol{X}\|$ represent the (m, n)th entry, the complex conjugate, the transpose, the Hermite transpose, the inverse, the trace and the Frobenius norm of $\boldsymbol{X}$, respectively. The operator $\mathrm{vec}[\cdot]$ denotes the vector-operation which aligns all columns of a matrix into a single column vector in a left-to-right fashion, and the operator $\otimes$ stands for the Kronecker product of two matrices. Given matrices $\boldsymbol{X}$, $\boldsymbol{Y}$, and $\boldsymbol{Z}$ of appropriate size, we can write $\mathrm{vec}[\boldsymbol{X}\boldsymbol{Y}\boldsymbol{Z}] = (\boldsymbol{Z}^{\mathrm{T}} \otimes \boldsymbol{X})\mathrm{vec}[\boldsymbol{Y}]$. The set of real numbers is denoted by $\mathbb{R}$.

II. Non-Coherent MIMO Transmission

A. Non-Coherent Block Transmission

We consider $M \times N$ MIMO systems in which M transmitting antennas and N receiving antennas are used. We focus on non-coherent communications where both the transmitter and the receiver do not have any knowledge of CSI. The use of non-coherent codes [22–29, 32–36] enables us to communicate efficiently even if no pilots and training sequences are used.

Let $\boldsymbol{x}_n \in \mathbb{C}^{M \times 1}$ be the signals vector transmitted from M antennas at the nth symbol. We assume L symbols long for a transmission block length of one codeword. Each block consists of $\boldsymbol{X} = [\boldsymbol{x}_1, \boldsymbol{x}_2, \ldots, \boldsymbol{x}_L] \in \mathbb{X} \subset \mathbb{C}^{M \times L}$, where $\mathbb{X} = \{\boldsymbol{\mathcal{X}}_1, \boldsymbol{\mathcal{X}}_2, \ldots, \boldsymbol{\mathcal{X}}_Q\}$ denotes a non-coherent space-time codebook with Q distinct codewords. Without losing generality, the mean energy of the codeword is set to be M, namely $Q^{-1} \sum_{q=1}^{Q} \|\boldsymbol{\mathcal{X}}_q\|^2 = M$.

Over the MIMO channels, the received signal is written as

$$\boldsymbol{y}_n = \boldsymbol{H}_n \boldsymbol{x}_n + \boldsymbol{w}_n, \tag{1}$$

where $\boldsymbol{y}_n \in \mathbb{C}^{N \times 1}$, $\boldsymbol{H}_n \in \mathbb{C}^{N \times M}$ and $\boldsymbol{w}_n \in \mathbb{C}^{N \times 1}$ denote the received signals vector, the MIMO channel matrix and the additive noise, respectively, at the nth symbol instance. In order to describe the conventional GLRT receiver [38], we first assume that the MIMO channel matrix remains static such that $\boldsymbol{H}_n = \boldsymbol{H}$ during a single block duration for $n = 1, 2, \ldots, L$ (this assumption will be relaxed later when we introduce a high-order codebook to deal with time-varying channels over a block length). This assumption of block fading channels simplifies the expression of the received signal into a matrix form as follows:

$$\boldsymbol{Y} = \boldsymbol{H}\boldsymbol{X} + \boldsymbol{W}, \tag{2}$$

where $\boldsymbol{Y}$ and $\boldsymbol{W}$ denote the received signals and the additive noise signals over the code block duration:

$$\boldsymbol{Y} = [\boldsymbol{y}_1, \boldsymbol{y}_2, \ldots, \boldsymbol{y}_L] \in \mathbb{C}^{N \times L}, \tag{3}$$

$$\boldsymbol{W} = [\boldsymbol{w}_1, \boldsymbol{w}_2, \ldots, \boldsymbol{w}_L] \in \mathbb{C}^{N \times L}. \tag{4}$$

We suppose that the noise is white Gaussian random variables: $\mathbb{E}[\mathrm{vec}[\boldsymbol{W}]\mathrm{vec}[\boldsymbol{W}]^\dagger] = \sigma^2 \boldsymbol{I}_{NL}$. Note that it is straightforward to consider a colored noise as discussed in [36].

B. Generalized Likelihood Ratio Test (GLRT) Blind Receiver

The conditional probability of $\boldsymbol{Y}$ given $\boldsymbol{X}$ and $\boldsymbol{H}$ is known as the likelihood which is expressed as

$$\mathrm{Pr}(\boldsymbol{Y} \mid \boldsymbol{X}, \boldsymbol{H}) = \frac{1}{(\pi\sigma^2)^{NL}} \exp\left(-\frac{1}{\sigma^2} \|\boldsymbol{Y} - \boldsymbol{H}\boldsymbol{X}\|^2\right). \tag{5}$$

Without CSI, the GLRT receiver [38] searches for the best estimate $\hat{\boldsymbol{X}}$ from the codebook $\mathbb{X}$ in favor of maximizing the likelihood, or equivalently minimizing the squared distance metric as follows:

$$\hat{\boldsymbol{X}} = \arg\min_{\boldsymbol{X} \in \mathbb{X}} \inf_{\boldsymbol{H}} \|\boldsymbol{Y} - \boldsymbol{H}\boldsymbol{X}\|^2. \tag{6}$$

Note that since $\boldsymbol{H}$ is not known at the receiver, the GLRT uses the best channel matrix over all the possible realizations for each codewords.

Since we have

$$\frac{\partial}{\partial \boldsymbol{H}^*} \|\boldsymbol{Y} - \boldsymbol{H}\boldsymbol{X}\|^2 = -(\boldsymbol{Y} - \boldsymbol{H}\boldsymbol{X})\boldsymbol{X}^\dagger, \tag{7}$$

the channel candidate $\hat{\boldsymbol{H}} = \boldsymbol{Y}\boldsymbol{X}^\dagger(\boldsymbol{X}\boldsymbol{X}^\dagger)^{-1}$ can maximize the likelihood, where we assume $\boldsymbol{X}\boldsymbol{X}^\dagger$ is invertible. This is equivalent to the well-known lest-squares (LS) channel estimation given a codeword candidate $\boldsymbol{X}$. Substituting $\hat{\boldsymbol{H}}$ for $\boldsymbol{H}$ in (6) yields

$$\hat{\boldsymbol{X}} = \arg\min_{\boldsymbol{X} \in \mathbb{X}} \left\| \boldsymbol{Y} \underbrace{\left(\boldsymbol{I}_L - \boldsymbol{X}^\dagger(\boldsymbol{X}\boldsymbol{X}^\dagger)^{-1}\boldsymbol{X}\right)}_{\boldsymbol{P}} \right\|^2. \tag{8}$$

If every codeword is unitary such that $\boldsymbol{\mathcal{X}}_q\boldsymbol{\mathcal{X}}_q^\dagger = \boldsymbol{I}_M$ for any $q = 1, 2, \ldots, Q$, the GLRT metric can be simplified to $\max \|\boldsymbol{Y}\boldsymbol{X}^\dagger\|^2$.

Here, a matrix $\boldsymbol{P} \in \mathbb{P} \subset \mathbb{C}^{L \times L}$ denotes an idempotent projector onto the orthogonal complement of a codeword $\boldsymbol{X}$;

bps/Hz	Q	k_1	k_2	k_3	Trace
1	4	1	0	0	0.71
2	16	7	2	0	0.71
3	64	14	5	0	0.49
4	256	104	14	0	0.32
5	1024	6	191	0	0.21
6	4096	732	1131	0	0.14

i.e., $\boldsymbol{XP} = \boldsymbol{0}$ and $\boldsymbol{PP} = \boldsymbol{P}$. The set $\mathbb{P} = \{\boldsymbol{\mathcal{P}}_1, \boldsymbol{\mathcal{P}}_2, \ldots, \boldsymbol{\mathcal{P}}_Q\}$ is a projector bank, whose qth member is defined as $\boldsymbol{\mathcal{P}}_q = \boldsymbol{I}_L - \boldsymbol{\mathcal{X}}_q^\dagger (\boldsymbol{\mathcal{X}}_q \boldsymbol{\mathcal{X}}_q^\dagger)^{-1} \boldsymbol{\mathcal{X}}_q$, for the codebook $\mathbb{X}$. The LQ factorization of $\boldsymbol{P}$ and the QR factorization of $\boldsymbol{Y}$ may be advantageous for reducing the computational complexity. It should be noted that the minimum size of the possible projector matrix $\boldsymbol{P}$ such that $\boldsymbol{XP} = \boldsymbol{0}$ can be $L \times (L - M)$ because the orthogonal complement of $\boldsymbol{X}$ is of size $L \times (L - M)$.

C. Non-Coherent Grassmann Codes

There are a number of non-coherent codes, e.g., unitary space-time codes [22–26, 28, 29, 31], Grassmann codes with exponential mapping [32, 33], Grassmann packing codes with numerical optimization [34–36] or operator Reed–Muller codes [37], and differential modulations [27]. All the different non-coherent codes can be viewed as a Grassmann code, i.e., ortho-normal sequences across different antennas. In [21], Yang *et al.* proved that Grassmann codes extended with Beta-distributed amplitudes achieve capacity in non-coherent massive MIMO communications although its gain over the Grassmann codes is marginal when the number of antennas is small.

In this paper, we use differential unitary product codes proposed in [31], where the kth unitary constellation is parameterized as follows:

$$\boldsymbol{X}_k = \begin{bmatrix} e^{j2\pi k/Q} & 0 \\ 0 & e^{j2\pi k_1 k/Q} \end{bmatrix} \cdot$$
$$\begin{bmatrix} \cos(2\pi k_2 k/Q) & \sin(2\pi k_2 k/Q) \\ -\sin(2\pi k_2 k/Q) & \cos(2\pi k_2 k/Q) \end{bmatrix} \begin{bmatrix} e^{j2\pi k_3 k/Q} & 0 \\ 0 & e^{-j2\pi k_3 k/Q} \end{bmatrix},$$
(9)

where Q is the maximum constellation cardinality, and $\{k_1, k_2, k_3\}$ are parameters to be optimized. We use the parameters listed in Table I, where we also present the trace metric to indicate the codeword distance for various spectral efficiencies up to 6 bps/Hz.

D. Motivations

In this paper, we focus on the use of MIMO-OFDM signaling to readily combat frequency-selective fading channels. For MIMO-OFDM systems, non-coherent codes are used over space and frequency dimensions rather than over space and time dimensions. From this context, non-coherent coding can be called space-frequency block coding (SFBC) rather than space-time block coding (STBC). Nevertheless, this paper does not strictly distinguish between STBC and SFBC since it is not important in principle for doubly-selective fading channels.

The conventional GLRT receivers cannot perform well in time-varying fading channels. In [39], the authors proposed improved GLRT using BEM and multi-symbol detection for such time-selective fading. In this paper, we further improve the method by introducing 2D-BEM for doubly-selective fading channels. In addition, we aim at achieving high-throughput non-coherent transmission achieving up to 6 bps/Hz.

There exist few literature, that demonstrated the realization of high-rate non-coherent communications achieving more than 2 bps/Hz. This is because signal constellations shall be mapped in Grassmannian manifold, i.e., on a surface of hypersphere, leading to smaller distance between signal points. For example in single-antenna systems, differential QPSK can realize non-coherent transmission to achieve 2 bps/Hz, whereas non-coherent modulation with differential 64PSK to achieve 6 bps/Hz can suffer from a severe penalty due to its small Euclidean distance compared to coherent 64QAM. Thus, achieving high-rate non-coherent transmission is challenging in particular for doubly-selective channels. We propose improved blind receivers to realize 6 bps/Hz non-coherent transmission for such wireless channels.

III. IMPROVED GLRT WITH 2D-BEM

A. Virtual Codebook and Improved Projector Bank

As shown in (8), the conventional GLRT receiver computes the metric $\|\boldsymbol{YP}\|^2$ with $\boldsymbol{P}$ being a member of the projector bank $\mathbb{P} = \{\boldsymbol{\mathcal{P}}_1, \boldsymbol{\mathcal{P}}_2, \ldots, \boldsymbol{\mathcal{P}}_Q\}$ which corresponds to the orthogonal complement of the transmitting codebook $\mathbb{X} = \{\boldsymbol{\mathcal{X}}_1, \boldsymbol{\mathcal{X}}_2, \ldots, \boldsymbol{\mathcal{X}}_Q\}$ such that $\boldsymbol{\mathcal{X}}_q \boldsymbol{\mathcal{P}}_q = \boldsymbol{0}$ for any $q \in \{1, 2, \ldots, Q\}$. The improved GLRT with a virtual codebook uses a modified projector bank $\mathbb{P}' = \{\boldsymbol{\mathcal{P}}'_1, \boldsymbol{\mathcal{P}}'_2, \ldots, \boldsymbol{\mathcal{P}}'_{Q'}\}$ which is generated from a virtual codebook $\mathbb{X}' = \{\boldsymbol{\mathcal{X}}'_1, \boldsymbol{\mathcal{X}}'_2, \ldots, \boldsymbol{\mathcal{X}}'_{Q'}\}$ not directly from the original transmitting codebook $\mathbb{X}$, where Q' is the cardinality of the virtual codebook.

As we will see, some virtual codebooks (super-block high-order codebooks) can significantly improve performance by dealing with some channel impairments such as time-varying fading over a coding block. Note that the actual transmitting signal remains the original codebook $\mathbb{X}$, whereas the receiver considers a virtual codebook $\mathbb{X}'$ as a transmitted codebook to generate a modified projector bank $\mathbb{P}'$ for performance improvement.

B. Super-Block GLRT

The length of the non-coherent codes L should be shorter than the coherence time in principle. However, shorter space-time codes have a poor performance with the conventional GLRT receiver. It is because the accuracy of the LS channel regressions decreases linearly with the code length L. Even for fast fading channels, the channel matrix has a high correlation for adjacent blocks in general. It suggests that we can enjoy a performance gain through the use of channel correlations when we increase the effective block length by coupling multiple blocks at receivers in low-selective channels.
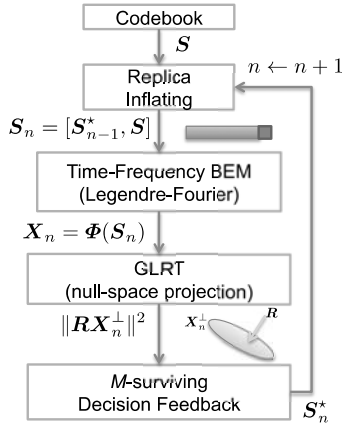
Fig. 1. Sequential GLRT with 2D-BEM.

We propose super-block GLRT receiver, which jointly estimates the adjacent K blocks. Let $\boldsymbol{X}_k$ and $\boldsymbol{Y}_k$ be the transmission block and the received block at the kth block for $k \in \{1, 2, \ldots, K\}$. When we write a super-block received signal and a super-block transmitted signal as

$$\boldsymbol{Y}' = [\boldsymbol{Y}_1, \boldsymbol{Y}_2, \ldots, \boldsymbol{Y}_K] \in \mathbb{C}^{N \times LK}, \qquad (10)$$

$$\boldsymbol{X}' = [\boldsymbol{X}_1, \boldsymbol{X}_2, \ldots, \boldsymbol{X}_K] \in \mathbb{C}^{M \times LK}, \qquad (11)$$

we can use the same procedure of GLRT receiver if the channel remains constant over the K blocks. Here, the signal $\boldsymbol{X}'$ is a super-block codeword generated from the original codebook $\boldsymbol{X}_k \in \mathbb{X}$. Note that the computational complexity increases exponentially with the number of blocks K because the cardinality of a super-block codebook becomes $Q' = Q^K$. If we use unitary codes, the GLRT metric reduces to $\max \| \sum \boldsymbol{Y}_k \boldsymbol{X}_k^{\dagger} \|^2$.

C. Linear-Complexity Sequential GLRT

Although super-block GLRT can improve performance by increasing block size of joint symbol detection, its main drawback lies in its exponentially increasing computational complexity. In order to reduce the computational complexity, we introduce a sequential GLRT, where the block size for multi-symbol detection is successively increased via Viterbi-like sequence detection with a finite number of surviving paths. Fig. 1 shows the schematic of the sequential GLRT, where we can make a reliable decision via maximum-likelihood sequence estimation (MLSE) method. Using M-algorithm, the computational complexity of super-block GLRT can be maintained in the linear order regardless of the block length. In addition, per-survivor processing to expand the basis can reduce the required memory size of virtual codebook.

D. High-Order GLRT

The GLRT receiver in principle requires an assumption that the channel remains static during a super block (or, consecutive LK symbols). Hence, a channel fluctuation during a block may incur a severe performance degradation. Here, we propose the use of high-order LS channel estimation [41] for GLRT receivers in order to overcome the channel variation during the

block. Let us use the Dth order polynomial curves to fit the channel fluctuation for high-order LS regressions. The channel matrix at the nth symbol is then modeled as follows:

$$\boldsymbol{H}_n = \sum_{d=0}^{D} \boldsymbol{H}^{[d]} n^d = \boldsymbol{\mathcal{H}} \boldsymbol{D}_n, \qquad (12)$$

where

$$\boldsymbol{\mathcal{H}} = [\boldsymbol{H}^{[0]}, \boldsymbol{H}^{[1]}, \ldots, \boldsymbol{H}^{[D]}] \in \mathbb{C}^{N \times M(D+1)}, \qquad (13)$$

$$\boldsymbol{D}_n = [n^0 \boldsymbol{I}_M, n^1 \boldsymbol{I}_M, \ldots, n^D \boldsymbol{I}_M]^{\mathrm{T}} \in \mathbb{R}^{M(D+1) \times M}. \quad (14)$$

The matrix $\boldsymbol{H}^{[d]}$ denotes the channel matrix at the dth order term of the polynomial for $d \in \{0, 1, \ldots, D\}$. This model enables us to adopt the GLRT receiver even when $\boldsymbol{H}_n$ is changing over symbols because the expanded channel matrix $\boldsymbol{\mathcal{H}}$ remains static.

The received signal can be rewritten as

$$\boldsymbol{Y} = \boldsymbol{\mathcal{H}} \underbrace{\boldsymbol{\mathcal{D}} \boldsymbol{\Lambda}}_{\boldsymbol{X}'} + \boldsymbol{W}, \qquad (15)$$

where $\boldsymbol{\mathcal{D}}$ is the (deterministic) order expansion matrix and $\boldsymbol{\Lambda}$ is the diagonally aligned version of the transmitted signal matrix $\boldsymbol{X}$, each of which is defined as

$$\boldsymbol{\mathcal{D}} = [\boldsymbol{D}_1, \boldsymbol{D}_2, \ldots, \boldsymbol{D}_{LK}] \in \mathbb{R}^{M(D+1) \times MLK}, \qquad (16)$$

$$\boldsymbol{\Lambda} = \begin{bmatrix} \boldsymbol{x}_1 & & & \\ & \boldsymbol{x}_2 & & \\ & & \ddots & \\ & & & \boldsymbol{x}_{LK} \end{bmatrix} \in \mathbb{C}^{MLK \times LK}. \qquad (17)$$

By considering $\boldsymbol{X}' = \boldsymbol{\mathcal{D}} \boldsymbol{\Lambda}$ as a new virtual codeword, the associated projector matrix becomes

$$\boldsymbol{P}' = \boldsymbol{I}_{LK} - \boldsymbol{\Lambda}^{\dagger} \boldsymbol{\mathcal{D}}^{\dagger} (\boldsymbol{\mathcal{D}} \boldsymbol{\Lambda} \boldsymbol{\Lambda}^{\dagger} \boldsymbol{\mathcal{D}}^{\dagger})^{-1} \boldsymbol{\mathcal{D}} \boldsymbol{\Lambda} \in \mathbb{C}^{LK \times LK}, \quad (18)$$

which can be computed in advance for $D = 0, 1, 2, \ldots$ and for all codewords. More importantly, the computational complexity of the high-order GLRT is independent of the order D because the modified projector matrix $\boldsymbol{P}'$ is size of LK. Note that there is a constraint on the maximum available order D; more specifically, $M(D+1) < LK$ must be fulfilled because $M(D+1) > LK$ results into the rank deficiency of the term $\boldsymbol{\mathcal{D}} \boldsymbol{\Lambda} \boldsymbol{\Lambda}^{\dagger} \boldsymbol{\mathcal{D}}^{\dagger}$ for any arbitrary codebook. This drawback can be dealt with by increasing the super-block length K. Obviously, higher-order modeling is advantageous only if the channel response frequently changes during a super-block.

E. Two-Dimensional Basis Expansion Model

In the above discussion, the BEM based on polynomial basis function was used for modeling time-varying channels. In fact, the optimal basis functions can be obtained by principal eigenvectors of auto-covariance matrix, according to Karhunen–Loève theorem (KLT). Fig. 2 shows the principal eigenvalues for time-varying fading channels, whose auto-correlation function is expressed by the modified Bessel function as $J_0(2\pi f_{\mathrm{D}} T_{\mathrm{s}} k)$ under the Jakes fading model. It can be seen that only a few eigenvectors are required to describe
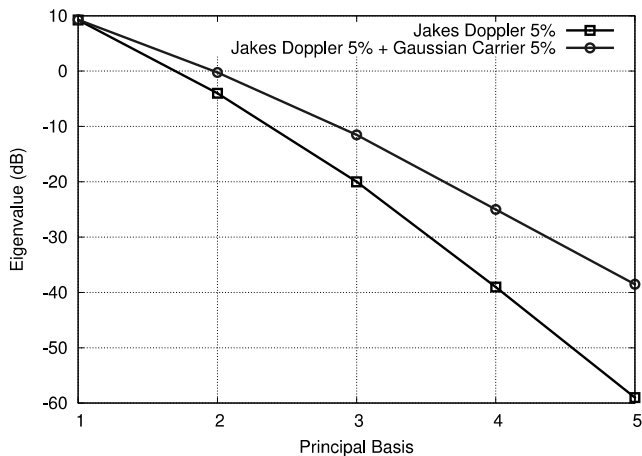
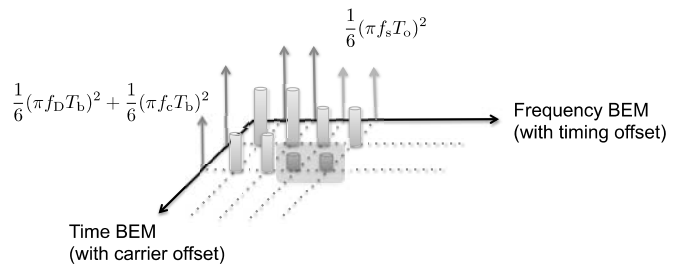Fig. 2. Eigenvalue of channel auto-correlation matrix.

Fig. 3. Spectral-temporal 2D-BEM with carrier frequency offset and timing offset for doubly-selective MIMO fading channels.

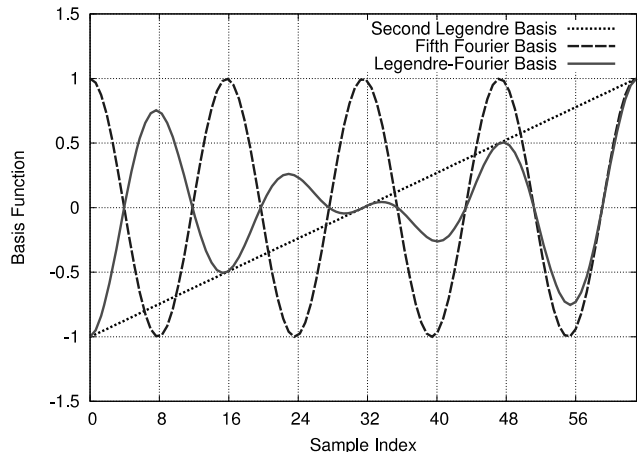Fig. 4. Fourier–Legendre basis with convolution to improve robustness against timing offset.

time-varying channels; more specifically, the third principal eigenvalue can be already negligible as it is $20\,\text{dB}$ lower than the first principal eigenvalue. It is found that the KLT basis of such auto-covariance matrix is nearly identical to discrete orthogonal Legendre polynomial (DOLP) for $f_\text{D}T_\text{s} \leq 10\%$. This is explained by a fact that the Bessel function is expressed as $J_0(x) = 1 - x^2/4 + x^4/64 + \mathcal{O}[x^6]$ for small x. It suggests that the Legendre basis can perform well for most symmetry auto-covariance matrices besides the Jakes Doppler spread. For example, the Gaussian-type auto-correlation function has $\exp(-x^2/2) = 1 - x^2/2 + x^4/8 + \mathcal{O}[x^6]$, corresponding to $3\,\text{dB}$ and $9\,\text{dB}$ larger eigenvalues than Bessel-type auto-correlation functions for the second and third principal components, respectively. In Fig. 2, we also present the eigenvalues for time-varying fading channels with 5% Doppler spread in the presence of 5% carrier frequency offset having Gaussian auto-correlation function. Since the carrier frequency offset effectively increases the Doppler spectrum, more basis functions may be required to describe the stochastic channels accurately.

Fig. 3 shows the principal component in doubly-selective fading channels via two-dimensional BEM, in which Legendre basis and Fourier basis are used to deal with Doppler spread and delay spread, respectively. As discussed, carrier frequency offset can be handled by increased Legendre basis, whereas timing offset requires modified Fourier basis functions. Considering the fact that most auto-correlation function can be approximated by Taylor series, we use Legendre basis to modify the Fourier basis by convolution as shown in Fig. 4. By using this robust Fourier–Legendre 2D basis, GLRT can allow high mobility and wideband signaling even in the presence of carrier frequency and timing offsets.

IV. PERFORMANCE EVALUATION

A. Simulation Parameter

We now evaluate the bit-error-rate (BER) performance for high-rate non-coherent MIMO transmission. The transmitter uses $M = 2$ antennas and the receiver uses $N = 2$ antennas.

The channel is assumed frequency-selective Rayleigh fading with an equal-gain power delay profile having 5% delay spread normalized by OFDM symbol duration. We consider the normalized maximum Doppler frequency of $f_\text{D}T_\text{s} = 5\%$. For block transmission, we use USTM based on unitary product codes [31] as listed in Table I, with OFDM signaling having 64 subcarriers. For evaluating hardware impairments, we also consider carrier frequency offset and timing offset. Although we evaluate uncoded BER performance, we assume the use of forward error correction (FEC) codes having the threshold of 2×10^{-3}, which is reasonable even for hard-decision low-overhead Reed–Solomon coding of high code rate 0.935 used in ITU-T G.975.1 [42].

B. BER Performance

Fig. 5 shows a benchmark performance of conventional GLRT and original high-order super-block GLRT with 1D-BEM [39] for various spectral efficiencies from 1 to 6 b/s/Hz. Because the original GLRT assumes time-invariant frequency-flat fading channels, the BER performance degrades significantly due to the strong interference, in particular for higher-order modulation. The interference causes severe error floors, which are above the FEC limit even for 1 bps/Hz case. The error floor is remarkably poor, i.e., near 0.5, for the cases of
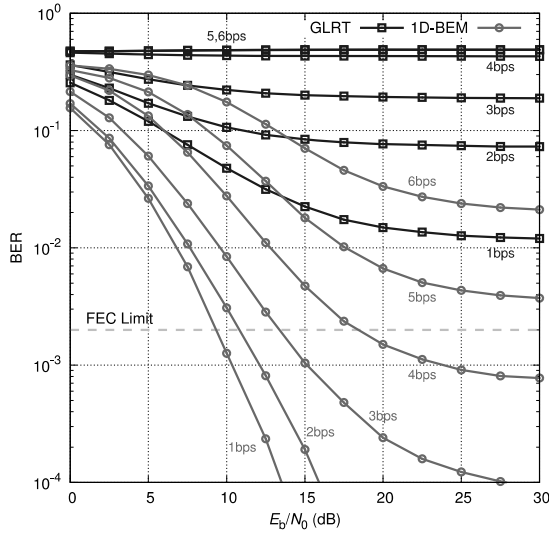
Fig. 5. BER performance of super-block high-order GLRT with 1D-BEM in doubly-selective fading channels.
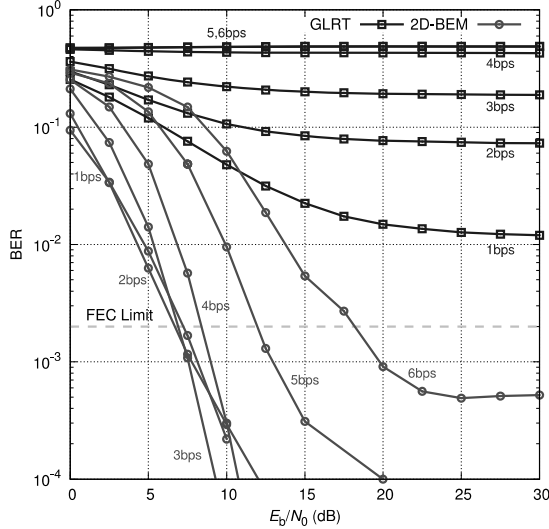

Fig. 7. BER performance as a function of timing offset at 8 dB for sequential GLRT with 2D-BEM and robust 2D-BEM for 3 bps/Hz.

Fig. 6. BER performance of sequential GLRT with 2D-BEM in doubly-selective fading channels.

Fig. 8. BER performance of sequential GLRT with robust 2D-BEM in presence of 2% carrier frequency offset and 10% timing offset.

5 and 6 bps/Hz. The super-block high-order GLRT using 1D-BEM [39] significantly improves the BER performance within the FEC limit for 1–4 bps/Hz. It indicates that realizing high-throughput non-coherent transmission is challenging even with improved blind receivers in doubly-selective fading channels. As shown in Fig. 6, our proposed sequential GLRT with 2D-BEM can achieve 6 bps/Hz transmission by improving the error floor significantly.

C. Carrier Frequency and Timing Offsets

Since the proposed 2D-BEM assumes perfect synchronization in time and frequency, the BER performance may be significantly degraded in the presence of carrier frequency
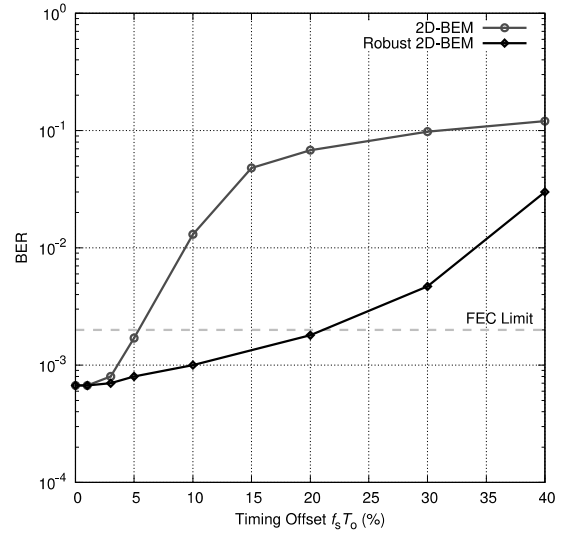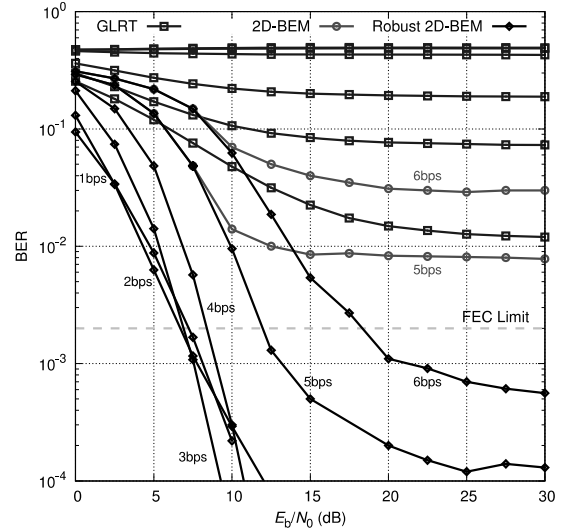
offset and timing offset. Fig. 7 plots the BER performance as a function of timing offset relative to the symbol duration for 2D-BEM GLRT with and without robust Fourier–Legendre product basis. We can observe that the proposed robust BEM shows a significant advantage in mitigating penalty caused by timing offset.

In Fig. 8, we present the BER performance of sequential GLRT with robust 2D-BEM in doubly-selective fading channels in the presence of 2% carrier frequency and 10% timing offsets. The 2D-BEM without robust basis now performs worse than the FEC limit for 6 b/s/Hz, whereas the proposed scheme with robust basis can still maintain the BER

performance under the FEC limit.

V. CONCLUSION

In this paper, we proposed a sequential GLRT receiver with time-frequency BEM for non-coherent MIMO transmission in doubly-selective fading channels. In order to be robust against hardware impairments including carrier frequency offset and timing offset, we also introduced a Fourier–Legendre convolution basis. It was demonstrated that the proposed method offers a significant improvement over the conventional GLRT receiver in the presence of strong interference in addition to carrier frequency and timing offsets, and that spectrally efficient non-coherent MIMO transmission achieving 6 bps/Hz can be realized without relying on any pilots.

ACKNOWLEDGMENT

REFERENCES

[1] G. J. Foschini, "Layered space-time architecture for wireless communication in a fading environment when using multi-element antennas," *Bell Labs. Tech. J.*, vol. 1, no. 2, pp. 41–59, 1996.

[2] I. E. Telatar, "Capacity of multi-antenna Gaussian channels," *Eur. Trans. Telecomm.*, vol. 10, no. 6, pp. 585–595, Nov. 1999.

[3] F. Rusek, D. Persson, B. K. Lau, E. G. Larsson, T. L. Marzetta, O. Edfors, F. Tufvesson, "Scaling up MIMO: Opportunities and challenges with very large arrays," *IEEE Sig. Proc. Mag.*, vol. 30, no. 1, pp. 40–60, Jan. 2013.

[4] E. G. Larsson, O. Edfors, F. Tufvesson, and T. L. Marzetta, "Massive MIMO for next generation wireless systems," *IEEE Commun. Mag.*, vol. 52, no. 2, pp. 186–195, Feb. 2014.

[5] G. D. Golden, G. J. Foschini, R. A. Valenzuela, and P. W. Wolniansky, "Detection algorithm and initial laboratory results using V-BLAST space-time communication architecture," *Electron. Lett.*, vol. 35, pp. 14–16, Jan. 1999.

[6] V. Tarokh, N. Seshadri, and A. R. Calderbank, "Space-time codes for high data rate wireless communication: Performance criterion and code construction," *IEEE Trans. Inf. Theory*, vol. 44, pp. 744–765, Mar. 1998.

[7] S. Alamouti, "A simple transmit diversity technique for wireless communications," *IEEE J. Select. Areas Commun.*, vol. 16, pp. 1451–1458, Oct. 1998.

[8] B. Hassibi and B. Hochwald, "High-rate codes that are linear in space and time," *IEEE Trans. Inf. Theory*, vol. 48, pp. 1804–1824, July 2002.

[9] T. L. Marzetta, "Blast training: Estimating channel characteristics for high-capacity space-time wireless," *37th Annual Allerton Conference on Communications, Control, and Computing*, Sept. 1999.

[10] B. Hassibi and B. M. Hochwald, "How much training is needed in multiple-antenna wireless links?," *IEEE Trans. Inf. Theory*, vol. 49, no. 4, pp. 951–963, 2003.

[11] T. L. Marzetta, "Noncooperative cellular wireless with unlimited numbers of base station antennas," *IEEE Trans. Wireless Commun.*, vol. 9, no. 11, pp. 3590–3600, Nov. 2010.

[12] J. Hoydis, S. ten Brink, and M. Debbah, "Massive MIMO in the UL/DL of cellular networks: How many antennas do we need?" *IEEE J. Sel. Areas Commun.*, vol. 31, no. 2, pp. 160–171, Feb. 2013.

[13] R. Müller, M. Vehkaperä, and L. Cottatellucci, "Blind pilot decontamination," *ITG Workshop on Smart Antennas*, Stuttgart, Mar. 2013.

[14] H. Q. Ngo and E. G. Larsson, "EVD-based channel estimations for multicell multiuser MIMO with very large antenna arrays," *IEEE Int. Conf. Acoustics, Speed, Sig. Proc. (ICASSP)*, Mar. 2012.

[15] A. Ashikhmin and T. L. Marzetta, "Pilot contamination precoding in multi-cell large scale antenna systems," *IEEE Int. Sym. Inform. Theory (ISIT)*, Cambridge, MA, July 2012.

[16] T. Marzetta and B. Hochwald, "Capacity of a mobile multiple-antenna communication link in Rayleigh flat fading," *IEEE Trans. Inf. Theory*, vol. 45, pp. 139–157, 1999.

[17] L. Zheng and D. N. C. Tse, "Communication on the Grassmann manifold: a geometric approach to the noncoherent multiple-antenna channel," *IEEE Trans. Inf. Theory*, vol. 48, no. 2, pp. 359–384, Feb. 2002.

[18] B. Hassibi and T. L. Marzetta, "Multiple-antennas and isotropically-random unitary inputs: The received signal density in closed-form," *IEEE Trans. Inf. Theoy*, vol. 48, pp. 1473–1484, 2002.

[19] B. Hochwald, T. Marzetta, and B. Hassibi, "Space-time autocoding," *IEEE Trans. Inf. Theory*, pp. 2761–2781, Nov. 2001.

[20] M. Brehler and M. K. Varanasi, "Asymptotic error probability analysis of quadratic receivers in Rayleigh fading channels with applications to a unified analysis of coherent and noncoherent space-time receivers," *IEEE Trans. Inf. Theory*, vol. 47, pp. 2383–2399, Sept. 2001.

[21] W. Yang, G. Durisi, and E. Riegler, "On the capacity of large-MIMO block-fading channels," *IEEE J. Sel. Areas Commun.*, vol. 31, no. 2, pp. 117–132, 2013.

[22] B. M. Hochwald and T. L. Marzetta, "Unitary space-time modulation for multiple-antenna communication in Rayleigh flat-fading," *IEEE Trans. Inf. Theory*, vol. 46, pp. 543–564, Mar. 2000.

[23] B. M. Hochwald, T. L. Marzetta, T. J. Richardson, W. Sweldens, and R. Urbanke, "Systematic design of unitary space-time constellations," *IEEE Trans. Inf. Theory*, vol. 46, no. 6, pp. 1962–1973, Sept. 2000.

[24] Y. Jing and B. Hassibi, "Unitary space-time modulation via Cayley transform," *IEEE Trans. Signal Proc.*, vol. 51, no. 11, pp. 2891–2904, Nov. 2003.

[25] B. M. Hochwald and B. Hassibi, "Cayley differential unitary space-time codes," *IEEE Trans. Inf. Theory*, vol. 48, no. 6, pp. 1485–1503, June 2002.

[26] B. Hochwald and W. Sweldens, "Differential unitary space-time modulation," *IEEE Trans. Commun.*, vol. 48, pp. 2041–2052, Dec. 2000.

[27] B. L. Hughes, "Differential space-time modulation," *IEEE Trans. Inf. Theory*, vol. 46, no. 7, pp. 2567–2578, Nov. 2000.

[28] V. Tarokh and H. Jafarkhani, "A differential detection scheme for transmit diversity," *IEEE J. Sel. Areas Commun.*, vol. 18, no. 7, pp. 1169–1174, July 2000.

[29] V. Tarokh and M. Kim, "Existence and construction of noncoherent unitary space-time codes," *IEEE Trans. Inf. Theory*, vol. 25, no. 8, pp. 3112–3120, Dec. 2002.

[30] T. Marzetta, B. Hassibi, and B. Hochwald, "Structured unitary space-time constellations," *IEEE Trans. Inf. Theory*, pp. 942–950, 2002.

[31] X. B. Liang and X. G. Xia, "Unitary signal constellations for differential space-time modulation with two transmit antennas: Parametric codes, optimal designs, and bounds," *IEEE Trans. Inf. Theory*, vol. 48, no. 8, pp. 2291–2322, 2002.

[32] I. Kammoun, A. M. Cipriano, and J.-C. Belfiore, "Non-coherent codes over the Grassmannian," *IEEE Trans. Wireless Commun.*, vol. 6, no. 10, pp. 3657–3667, Oct. 2007.

[33] I. Kammoun and J. Belfiore, "A new family of Grassmann space-time codes for non-coherent MIMO systems," *IEEE Commun. Lett.*, vol. 7, no. 11, pp. 528–530, Nov. 2003.

[34] M. J. Borran, A. Sabharwal, and B. Aazhang, "On design criteria and construction of non-coherent space-time constellations," *IEEE Trans. Inf. Theory*, vol. 49, no. 10, pp. 2332–2351, Oct. 2003.

[35] M. Beko, J. Xavier, and V. Barroso, "Codebook design for the non-coherent GLRT receiver and low SNR MIMO block fading channel," *IEEE SPAWC*, Cannes, France, 2006.

[36] M. Beko, J. Xavier, and V. Barroso, "Codebook design for non-coherent communication in multiple-antenna systems," *IEEE ICASSP*, Toulouse, France, 2006.

[37] A. Ashikhmin and A. R. Calderbank, "Grassmannian packings from operator Reed-Muller codes," *IEEE Trans. Inf. Theory*, vol. 56, no. 11, Nov. 2010.

[38] S. Gaulliou, I. Kammoun, and J. Belfiore, "Space-time codes for the GLRT noncoherent detector," *IEEE ISIT*, 2002.

[39] T. Koike-Akino and P. Orlik, "High-order super-block GLRT for non-coherent Grassmann codes in MIMO-OFDM systems," *IEEE GLOBECOM*, Miami, Dec. 2010.

[40] G. B. Giannakis and C. Tepedelenlioglu, "Basis expansion models and diversity techniques for blind identification and equalization of time-varying channels," *IEEE*, vol. 86, no. 10, pp. 1969–1986, Oct. 1998.

[41] T. Koike-Akino, A. F. Molisch, M.-O. Pun, R. Annavajjala, and P. Orlik, "Order-extended sparse RLS algorithm for doubly-selective MIMO channel estimation," *IEEE ICC*, Kyoto, June 2011.

[42] ITU-T Recommendation G.975.1, 2004